A Single Stage Boost Converter for Body Heat Energy Harvesting with Maximum Power Point Tracking and Output Voltage Regulation

Quinn Brogan and Dong Sam Ha
Multifunctional Integrated Circuits and Systems (MICS) Group
Bradley Department of Electrical and Computer Engineering
Virginia Tech, Blacksburg, Virginia, 24061, USA
{quinn22, ha}@vt.edu

***Abstract*— The proposed circuit aims to harvest energy from body heat, in which the thermal gradient is only a few degrees. The boost converter operating in a burst mode offers a high conversion ratio while minimizing power loss. Maximum power point tracking based on the fractional open circuit voltage method ensures that the proposed circuit can be applied for a variety of thermoelectric generators (TEGs) and TEG setups. The proposed circuit is designed and laid out in CMOS 0.25 μm technology. Post layout simulation results indicate the converter is able to boost input voltages as low as 50 mV to the regulated output of 3 V, while achieving peak efficiency of 81%.**

Keywords*— Body heat energy harvesting, maximum power point tracking, boost converter, burst mode, thermoelectric generator.

I. Introduction

Thermoelectric energy generators (TEGs) convert thermal energy into electrical energy in the form of DC voltage. The energy generated by TEGs is small for small temperature gradients including body heat. Extensive research on circuit design has been conducted to harvest small thermal energy generated by TEGs [1]-[17]. As a TEG generates a low DC voltage from small thermal energy, there are several typical issues for the circuit design, specifically design of power management circuits.

First, it is often necessary to step up the voltage to power devices. A DC-DC converter or charge pump could be used for the purpose. An alternative approach is to design the load device for ultralow voltage and power [18]. In addition, regulation of the output voltage would be necessary for practical purposes. Second, the source impedance of TEGs depends on the construction of TEGs [19],[20]. To transfer the maximum power from a TEG to the load, the source impedance of the TEG should match the input impedance of the power management circuit. It is desirable for a circuit to match the source impedances of a given TEG without manual tuning. Then, the circuit is ready to work with TEGs with different source impedances. Adoption of maximum power point tracking (MPPT) serves the purpose. Lastly, power dissipation of the circuits should be minimized to increase the conversion efficiency.

A straightforward approach to address the first two isssues is to adopt two power stages in cascade; the first stage for MPPT and the second stage for output voltage regulation. Two power stages, however, dissipate large power, while increasing the circuit complexity.

A single stage converter that regulates both input and output voltages was proposed to harvest solar energy [21]. The converter uses a dual comparator scheme with MPPT based on the Fractional Open Circuit Voltage (FOCV) method. The converter is synchronous and adopts a constant on-time and adaptive off-time scheme, which increases the circuit complexity and hence power dissipation. Further, the converter operation is interrupted periodically to sample and hold the open circuit voltage [21]. We propose to address the shortcomings of the circuit through adoption of an asynchronous converter and a burst mode scheme. It reduces the circuit complexity to decrease power dissipation, resulting high efficiency, which is critical for the target application, body heat energy harvesting.

The proposed circuit aims to power wearable devices through body heat energy harvesting. The paper is organized as follows. Section II provides preliminaries including thermoelectric generators. Section III describes design and operation of key building blocks. Section IV presents simulation results, and Section V concludes the paper.

II. Preliminaries

A. Energy Harvesting with Thermoelectric Generators

A thermopile is n-type material in series with p-type. A TEG is composed of multiple thermopiles in parallel and/or series [22]. A TEG can be modeled as a DC voltage source in series with an internal resistance. The resistance can range from less than 1 Ω to several hundreds ohms [19],[20]. TEGs can only produce a few tens of mV from body heat due to the low temperature gradient [19]. So, it is necessary to step up the TEG voltage to power typical wearable devices such as wireless sensor nodes.

B. Boost Converter

While both the boost and buck-boost topologies work for the target application, a boost converter offers higher efficiency. A boost converter operating in discontinuous conduction mode (DCM) is adopted for the proposed circuit. The power stage of a boost converter and the DCM operation is shown in Fig. 1. During the D_1T_S period the NMOS is turned on, the input voltage charges the inductor L and the inductor current I_L rises.

The NMOS is turned off during the D_2T_S period, and I_L starts to decrease, and the current flows into the output capacitor. The load. I_L falls to zero during the D_3T_S period, and the diode is reverse biased to block the reverse current flow.

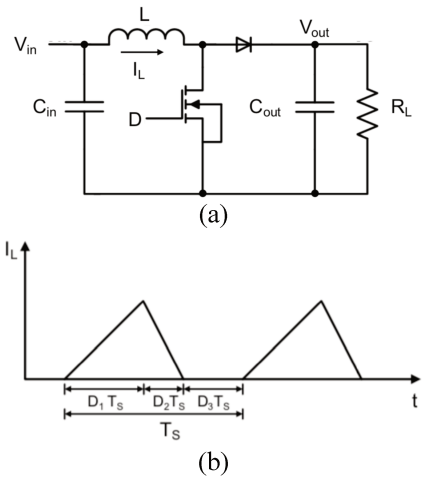

Fig. 1. Boost converter (a) circuit diagram (b) DCM operation.

The emulated input resistance of a boost converter in DCM is as follows [23].

$$R_{in\_Boost} = \frac{2L}{D_1^2 T_s}\left(1 - \frac{V_{in}}{V_{out}}\right) \quad (1)$$

R_{in_Boost} is dependent on the input and output voltages of the converter as well as other parameters. The conversion ratio V_{out}/V_{in} of the converter varies during the operation, and hence the input resistance R_{in_Boost}. The dependency of the resistance on the operation condition is reduced for high conversion ratios. However, a high conversion ratio leads to low efficiency of the converter, which is a drawback.

C. FOCV

The FOCV method used to implement MPPT relies on measurement of the open circuit voltage instead of the source resistance, and the open circuit voltage is often easier to measure than the source impedance during the operation [11]. Consider a TEG with the source voltage V_{TEG} in series with the source resistance R_{TEG}. Suppose that the TEG is connected to a load resistor R_{Load}. An MPPT circuit based on the FOCV method disconnects the load resistance R_{Load} periodically and measures the open circuit voltage V_{TEG} of the TEG. Then, it adjusts R_{Load} to set the voltage across R_{Load} to $0.5V_{TEG}$.

Now, suppose that the boost converter in Fig. 1 is connected to the TEG. In other words, the input resistance R_{in_Boost} effectively becomes the load resistor as far as the TEG is concerned. So the effective load resistance R_{in_Boost} is adjusted to set the input voltage V_{in} of the booster converter to be $0.5V_{TEG}$. However, as R_{in_Boost} is dependent on the input and output voltages of the converter as shown in (1), it is not guaranteed that R_{in_Boost} is equal to the source resistance R_{TEG}. So, the FOCV method could fail. As noted earlier, the dependency becomes less for a higher conversion ratio, and it is the case for the proposed circuit.

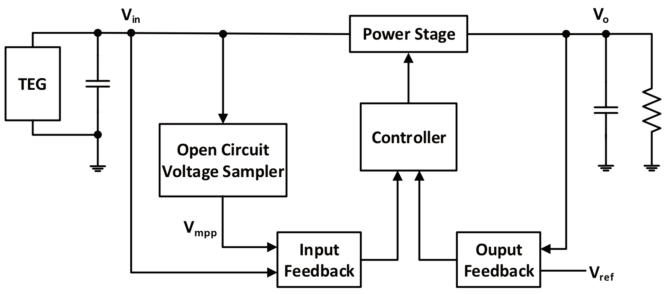

Fig. 2. Block diagram of the proposed circuit.

III. Proposed Energy Harvesting Circuit

The major control blocks of the proposed circuit are shown in Fig. 2. The proposed boost converter adopts a burst mode control to regulate output voltage [12]. During a burst period the output voltage V_o is regulated to the reference voltage V_{ref} via the output feedback loop. Also, the input voltage V_{in} is regulated to the maximum power point voltage V_{mpp} through the input feedback loop. Note that V_{mpp} is ideally one half of the open circuit voltage or $0.5V_{TEG}$, obtained through the FOCV method.

A. Operation Mode and Output Voltage Regulation

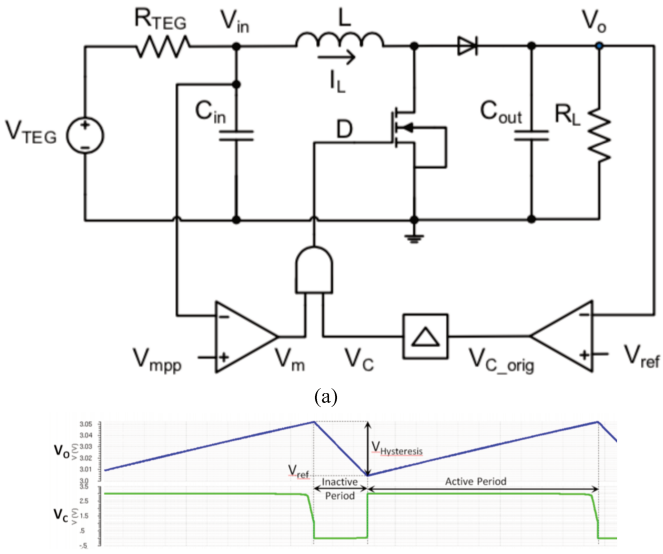

Fig. 3. Boost controller (a) simplified schematic diagram; (b) voltage waveforms.

Fig. 3 shows a schematic diagram of the boost converter with its controller and relevant waveforms. When the output voltage V_o falls below V_{ref}, the signal V_{C_orig} changes to high first and then followed by V_C after Δ delay. As V_C becomes high, the circuit moves into an "active" period. The boost converter starts switching according to the gate drive value of D, and the output voltage V_o starts to increase. Once V_o reaches $V_{ref} + V_{Hysteresis}$, where $V_{Hysteresis}$ is the hysteresis voltage of the comparator, V_c goes low and the circuit goes into an "inactive" period. The NMOS transistor is turned off, and the booster converter stops switching. As the TEG voltage V_{TEG} charges only the input capacitor C_{in}, the output voltage V_o starts to decrease. When V_o reaches below V_{ref}, the circuit moves into an active period, and repeats the same cycle. Hence, the output voltage V_o is regulated to V_{ref} with the voltage ripple of $V_{Hysteresis}$. The waveforms of V_o

and V_c are shown in Fig. 3 (b). The delay Δ is set to 50 µs for the proposed circuit and $V_{Hysteresis}$ to around 50 mV.

As the circuit enters an inactive period, *the NMOS transistor is turned off,* and the inductor current I_L charges the output capacitor C_{out}. The inductor current falls to zero eventually, and *the diode becomes reversed biased or is turned off.* The load (both C_{out} and R_L) is disconnected from the TEG. Now, the TEG voltage V_{TEG} charges only the input capacitor C_{in}, and the input voltage V_{in} rises toward the TEG voltage V_{TEG}. Once, C_{in} is fully charged, the input voltage V_{in} is equal to the open circuit voltage of the TEG or V_{TEG}. It is imperative to choose an input capacitor C_{in}. small enough to allow V_{in} to rise to the open circuit voltage even for the smallest inactive period.

B. Sampler for the Open Circuit Voltage

The sampler for the open circuit voltage is shown in Fig. 4. The capacitance of C_1 and C_2 is the same for the circuit. As V_o falls below V_{ref}, the signal V_{C_orig} changes to high, which signals end of the inactive period. It triggers the "Discharge" signal to be high for a short period, which in turn triggers the "Charge" signal. Hence, both capacitors C_1 and C_2 are discharged first, and then charged with the input voltage V_{in}. The maximum power point voltage V_{mpp} becomes $0.5V_{in}$, and the input voltage V_{in} is equal to the open circuit voltage provided the inactive period is sufficiently long. Finally, V_C becomes high after Δ delay, which moves the circuit into the active mode. The boost converter starts switching according to the gate drive value of D in Fig. 3.

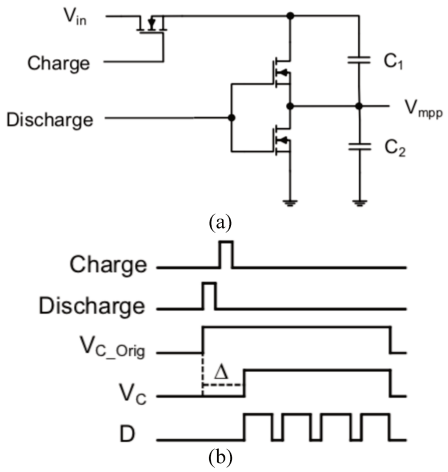

Fig. 4. Sampler for the open circuit voltage (a) circuit (b) singal waveforms.

C. Input Voltage Control during Active Periods

The output voltage V_o is above the target voltage V_{ref} during an inactive period, which implies the output capacitor is already charged fully. Hence, maximum extraction of energy from the TEG through MPPT is not critical for inactive periods. Hence, MPPT is performed only during active periods for the proposed circuit. The MPPT based on the FOCV method requires the input voltage V_{in} to be one half of the open circuit voltage or V_{mpp} in Fig. 4(a). A bang-bang control referenced to V_{mpp} is adopted for the proposed circuit, and relevant waveforms are shown in Fig. 5. Refer to Fig. 3 for the notations of the signals and voltages.

Consider the circuit is in an active period or V_C is high, Suppose the gate drive signal D switches from low to high. The NMOS transistor is turned on. The inductor current I_L begins to rise and resultantly V_{in} begins to fall. The TEG energy is transferred to the inductor. When V_{in} falls below V_{mpp}, the comparator output voltage V_m and hence the signal D go low, and the transistor is turned off. The inductor current I_L starts to fall, and I_L supplies energy to the load R_L and the output capacitor C_{out}, resulting in increase of the output voltage V_o. While I_L starts to fall, V_{in} starts to rise. Due to the hysteresis of the input comparator, V_m and hence D remain low until V_{in} crosses the V_{mpp} + $V_{Hysteresis}$ threshold. The inductor current reaches to zero eventually, the diode is reverse biased to block the reverse current flow. As the NMOS transistor remains turned off, the TEG charges only the input capacitor C_{in}. to increase V_{in} As V_{in} becomes greater than V_{mpp} + $V_{Hysteresis}$, V_m rises to high and hence D. The NMOS transistor is turned on to repeat the same cycle. It repeats until the end of the active period, equally V_o becomes greater than V_{ref} + $V_{Hysteresis}$. Hence, the input voltage is regulated to $V_{mpp} < V_{in} < V_{mpp} + V_{Hysteresis}$ or the optimum voltage of $0.5V_{TEG}$. The ripple $V_{Hysteresis}$ is set to around 50 mV for the proposed design.

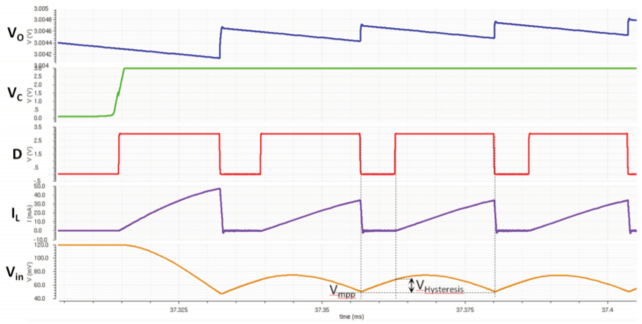

Fig. 5. Waveforms relevant to the input voltage.

IV. Layout and Simulation Results

A. Layout

The proposed circuit is designed and laid out in 0.25 µm CMOS technology. The layout of the analog and digital control blocks and relevant references, along with the power stage MOSFET, is shown in Fig. 6. The core die area of the chip, excluding pads, is 0.75 mm × 0.5 mm. The off-chip components include the diode, input capacitor (=5 µF), output capacitor (=2.2 µF), and inductor (=33 µH).

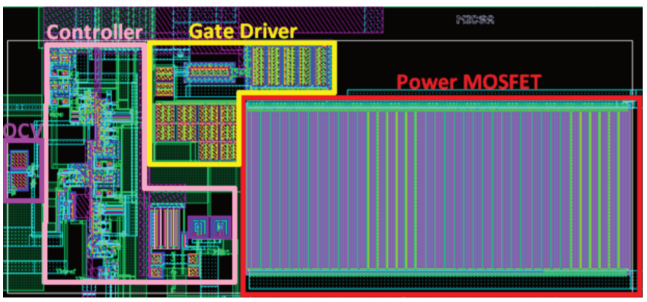

Fig. 6. Layout of the circuit.

B. Simulation Results

Post layout simulations are performed for the proposed circuit. For all simulations, the output capacitor C_{out} is pre-

charged to 3.1 V to be able to start the controller. The reference voltage V_{ref} is set to 3 V, which aims to regulate the output voltage to 3 V.

Simulation results for two different TEG voltages, 50 mV and 500 mV, are shown in Fig. 7. The converter sets the input voltage V_{in} at the maximum power point during active periods, i.e., V_{in} is regulated to about 27 mV for V_{TEG} = 50 mV and about 225 mV for V_{TEG} = 500 mV. It implies MPPT is performed with reasonable accuracy during active periods. The output voltage V_o can be regulated to 3 V for the input voltages as low as 50 mV, in which the conversion ratio of the boost converter is 60.

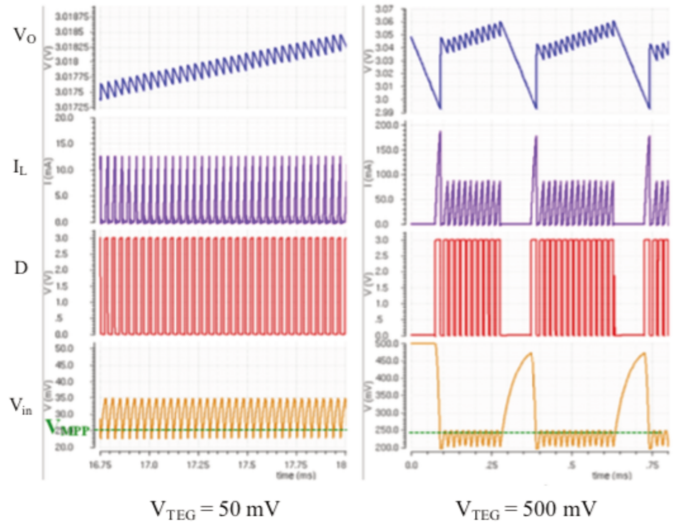

Fig. 7. Waveforms for V_{TEG} = 50 mV and 500 mV.

When the peak V_o voltage is about 60 mV above the target regulated output voltage (= 3 V) for V_{TEG} = 500 mV, the circuit moves into an inactive period to result in rapid decrease of V_o. It results in a sharp rise of the input voltage V_{in} during the inactive period. The peak V_{in} is about 475 mV, which is slightly lower than the open circuit voltage of 500 mV. It explains why V_{in} is regulated to slightly below the maximum power point of 250 mV. When V_o falls slightly below 3 V, the circuit returns to an active period.

Since the TEG voltage and energy delivered to the load are directly related, the converter adjusts the switching frequency and the duty cycle accordingly. As V_{TEG} increases from 50 mV to 500 mV, we observed that the switching frequency increases from 27 kHz to 56 kHz and the duty cycle D_1 from 0.37 to 0.69.

We also observed that active periods are much longer for lower TEG voltages. It is expected as the circuit takes longer time to reach the target regulated output voltage of 3 V for a lower TEG voltage. For example, the active period is 80 ms for V_{TEG} = 50 mV, compared to just 0.35 ms for V_{TEG} = 500 mV. Through simulations, we realized that the designed sampler for open circuit voltage fails to work for long active periods; the current laid out circuit requires off-chip capacitors to increase accuracy.

The efficiency of the proposed circuit for R_{TEG} = 1 Ω is shown in Fig. 8. The efficiency increases as the TEG voltage increase initially and decreases after hitting the peak value of 81% under V_{TEG} = 300 mV. The proposed circuit achieves over 78% of efficiency over the entire TEG voltage range owing to adoption of MPPT.

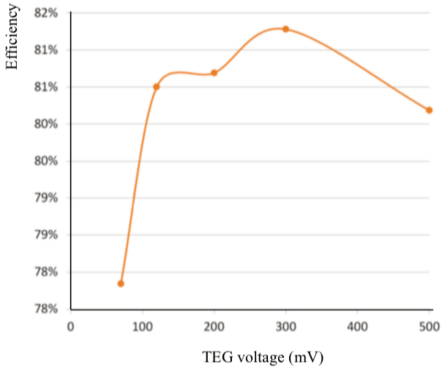

Fig. 8. Efficiency versus the TEG voltage.

C. *Comparison with Other Works*

Table 1 compares the performance of relevant works for thermal energy harvesting and the proposed circuit. It is difficult to make a fair comparison of the performance due to differences such as processing technology, TEG type, adoption of MPPT, input and output power level, and output voltage. The proposed circuit and [12] achieve higher peak efficiency than the other two circuits. The proposed circuit adopts MPPT, while [12] does not. Adoption of MPPT makes the proposed circuit to achieve high efficiency over a wide input voltage range. One shortcoming of the proposed circuit is a high minimum input voltage.

TABLE 1. COMPARISON OF RECENT THERMAL ENERGY HARVESTING CIRCUITS

	Ahmed [12]	Ogawa [6]	Wang [9]	This Work
CMOS Technolology	0.13 µm	0.13 µm	0.18 µm	0.25 µm
Minimum V_{in}	12 mV	20 mV	50 mV	50 mV
Output Voltage	0.66 - 3.3 V	4.2 V	1.2 V	3 V
Peak Efficiency	82%	49%	63% *	81% *
MPPT	No	No	Yes	Yes
Cold-start	No	NA	RF kick-start	No

* It is for a simulation result.

V. CONCLUSION

An energy harvesting circuit for body heat is presented in this paper. The proposed circuit adopts a single stage boost converter operating in a burst mode. MPPT based on the FOCV method ensures that the proposed circuit can be applied for a variety of TEGs and TEG setups. The circuit was designed and laid out in 0.25 µm CMOS technology. Post layout simulation results validate correct operation of the converter and high efficiency. The minimum input voltage is 50 mV for the circuit, and so it would be able to harvest energy form body heat.

ACKNOWLEDGMENT

This research was supported in part by the National Science Foundation Award no 1704176.

References

[1] J. Mu and L. Liu, "A 12 mV Input, 90.8% Peak Efficiency CRM Boost Converter With a Sub-Threshold Startup Voltage for TEG Energy Harvesting," *IEEE Transactions on Circuits and Systems I: Regular Papers*, vol. 65, no. 8, pp. 2631 – 2640, Aug. 2018.

[2] J. Li, J.H. Hyun, and D.S. Ha, "A Multi-Source Energy Harvesting System to Power Microcontrollers for Cryptography," 44th Annual Conference of the IEEE Industrial Electronics Society (IECON 2018), pp. 901-906, Oct. 2018.

[3] J.H. Hyun, L. Huang, and D.S. Ha, "Vibration and Thermal Energy Harvesting System for Automobiles with Impedance Matching and Wake-up," International Symposium on Circuits and Systems (ISCAS), 5 pages, May 2018.

[4] A. Das, Y. Gao and T. T. Kim, "A 220-mV Power-on-Reset Based Self-Starter With 2-nW Quiescent Power for Thermoelectric Energy Harvesting Systems," *IEEE Transactions on Circuits and Systems I: Regular Papers*, vol. 64, no. 1, pp. 217-226, Jan. 2017.

[5] M. Guan et al, "A High Efficiency Boost Converter with MPPT Scheme for Low Voltage Thermoelectric Energy Harvesting," *Journal of Electronic Materials*, vol. 45, (11), pp. 5514-5520, Nov. 2016.

[6] T. Ogawa, T. Ueno, T. Miyazaki and T. Itakura, "20 mV input, 4.2 V output boost converter with methodology of maximum output power for thermoelectric energy harvesting," IEEE Applied Power Electronics Conference and Exposition (APEC), pp. 1907-1910, Mar. 2016.

[7] M. Ashraf and N. Masoumi, "A Thermal Energy Harvesting Power Supply With an Internal Startup Circuit for Pacemakers," *IEEE Transactions on Very Large Scale Integration (VLSI) Systems*, vol. 24, no. 1, pp. 26-37, Jan. 2016.

[8] M. Saida, G. Zaibi, M. Samet and A. Kachouri, "Improvement of energy harvested from the heat of the human body," 17th International Conference on Sciences and Techniques of Automatic Control and Computer Engineering (STA), Sousse, pp. 132-137, Dec. 2016.

[9] C. Wang, Z. Li, K. Zhao and Q. Guo, "Efficient self-powered converter with digitally controlled oscillator-based adaptive maximum power point tracking and RF kick-start for ultralow-voltage thermoelectric energy harvesting," *IET Circuits, Devices & Systems*, vol. 10, no. 2, pp. 147-155, Mar. 2016.

[10] A. K. Sinha, R. L. Radin, D. D. Caviglia, C. G. Montoro and M. C. Schneider, "An energy harvesting chip designed to extract maximum power from a TEG," IEEE 7th Latin American Symposium on Circuits & Systems (LASCAS), Florianopolis, pp. 367-370, Mar. 2016.

[11] A. Montecucco and A. R. Knox, "Maximum Power Point Tracking Converter Based on the Open-Circuit Voltage Method for Thermoelectric Generators," *IEEE Transactions on Power Electronics*, vol. 30, no. 2, pp. 828-839, Feb. 2015.

[12] K. Z. Ahmed and S. Mukhopadhyay, "A Wide Conversion Ratio, Extended Input 3.5- μA Boost Regulator With 82% Efficiency for Low-Voltage Energy Harvesting," *IEEE Transactions on Power Electronics*, vol. 29, no. 9, pp. 4776–4786, Sept. 2014.

[13] Q. Brogan, T. O'Connor, and D.S. Ha, "Solar and Thermal Energy Harvesting with a Wearable Jacket," International Symposium on Circuits and Systems (ISCAS), pp. 1412 – 1425, June 2014.

[14] K. Z. Ahmed and S. Mukhopadhyay, "A Wide Conversion Ratio, Extended Input 3.5μA Boost Regulator With 82% Efficiency for Low-Voltage Energy Harvesting," *IEEE Transactions on Power Electronics*, vol. 29, no. 9, pp. 4776–4786, Sept. 2014.

[15] J. Kim and C. Kim, "A DC-DC Boost Converter With Variation-Tolerant MPPT Technique and Efficient ZCS Circuit for Thermoelectric Energy Harvesting Applications," *IEEE Transactions on Power Electronics*, vol. 28, no. 8, pp. 3827–3833, Aug. 2013.

[16] P. S. Weng, H. Y. Tang, P. C. Ku and L. H. Lu, "50 mV-Input Batteryless Boost Converter for Thermal Energy Harvesting," *IEEE Journal of Solid-State Circuits*, vol. 48, no. 4, pp. 1031-1041, Apr. 2013.

[17] J. Kim and C. Kim, "A DC–DC Boost Converter with Variation-Tolerant MPPT Technique and Efficient ZCS Circuit for Thermoelectric Energy Harvesting Applications," *IEEE Transactions on Power Electronics,* vol. 28, no. 8, pp. 3827-3833, Aug. 2013.

[18] H. Yi, W. Yu, P. Mak, J. Yin and R. P. Martins, "A 0.18-V 382-μW Bluetooth Low-Energy Receiver Front-End With 1.33-nW Sleep Power for Energy-Harvesting Applications in 28-nm CMOS," *IEEE Journal of Solid-State Circuits*, vol. 53, no. 6, pp. 1618-1627, June 2018.

[19] "THERMOELECTRIC GENERATOR (TEG) MODULES," Online, RMT, LTD. [Online]. Available: https://www.marlow.com/products/power-generators/thermoelectric-generator-teg-modules

[20] "Thin Film Thermogenerator: MPG-D655 Preliminary Datasheet," Online, micropelt. [Online]. Available: https://docplayer.net/21473338-Mpg-d655-thin-film-thermogenerator-preliminary-datasheet.html

[21] S. Liu, Y. Zhao, M. Zhao, H. Zhang, and X. Wu, "A burst-mode based boost converter harvesting photovoltaic energy for low power applications," IEEE 57th International Midwest Symposium on Circuits and Systems (MWSCAS), pp. 49–52, Aug. 2014.

[22] Q. Wan, Y. K. Teh, Y. Gao and P. K. T. Mok, "Analysis and Design of a Thermoelectric Energy Harvesting System With Reconfigurable Array of Thermoelectric Generators for IoT Applications," *IEEE Transactions on Circuits and Systems I: Regular Papers*, vol. 64, no. 9, pp. 2346-2358, Sept. 2017.

[23] Y. Roshan and M. Moallem, "Maximum power point tracking using boost converter input resistance control by means of Lambert W-Function." IEEE International Symposium on Power Electronics for Distributed Generation Systems (PEDG), pp.195-199, June 2012.